AN *FCC* METASTABLE PHASE IN A RS Ni-Ti ALLOY[①]

Wu, Xiaozhen Wang, Shidong Zhang, Jinping Shu, Huaqin
Analytic and Testing Center, Southeast University, Nanjing 210018
Jin, Jialing Zhang, Jingguo
Shanghai Iron and Steel Institute, Shanghai 200940

ABSTRACT

An *fcc* metastable phase was first found in the rapidly solidified (RS) Ni-Ti SMA strip prepared by single roller melt spinning method. The lattice constant a_0 of this phase is 4.300 Å. Its composition is the same as that of the matrix, and it is also composed of near-equiatomic Ni and Ti. The morphology, distribution and formation mechanism of this phase were analysed and discussed.

Key words: rapid solidification Ni-Ti alloy *fcc* metastable phase morphology distribution formation mechanism

1 INTRODUCTION

Being an excellent shape memory alloy (SMA), the Ni-Ti alloy has been finding wide applications. However, the high working cost of small cross-section wires and strips made of this alloy, resulting from its bad workability, limits its further expanded applications. In order to solve this problem, researchers at home and abroad have taken great pains to adopt completely new technological processes to prepare this alloy. And the rapid solidification process is one of the important directions.

Up till now, much work has been reported on the structures of the matrix and the Ni-rich precipitates in the Ni-Ti alloys prepared by traditional technologies [1-6]. But little work has been done on the morphologies and structures of the Ni-Ti SMA under rapid solidification. Wood *et al*[7] found that the structure of the melt-spun Ni-Ti SMA matrix at room temperature remains the same as that under common solidification conditions, namely B_2 structure. This paper aims to further analyse the morphologies and structures of the RS Ni-Ti SMA.

2 EXPERIMENTAL

In this study, the vacuum single roller melt spinning method was used to prepare the RS Ni-Ti alloy strips. The composition of the master alloy was Ti-50.8at.-%Ni. And about 20g of the alloy for each test was melted in a quartz boron-nitride composite crucible. The $d230$ cooling roller was made of pure copper. Its rate in preparing the samples was 21 m/s. The whole process was conducted under an aeration of 1.36 MPa argon after a vacuity of 10^{-3} MPa was reached. The thickness and width of the samples were 0.05～0.07 μm, 5～6 mm respectively. And the cooling rate was about 2×10^5 K/s.

The cross-section morphologies of strips were observed on a HITACHI X－650 SEM; the etching medium was $8HF\text{-}15HNO_3\text{-}77H_2O$ (Vol.-%). The TEM observations were made on a JEM-2000 EX transmitting electron microscope with Link860 energy spectrum accessory; the electrolyte composition was $20H_2SO_4\text{-}80CH_3OH$, the polishing temperature was about －20 ℃, and the operation voltage was 15～20 V. A REGAKU K/MAX target rotating diffractometer was used to determine the

① Chinese mauscript received Jan. 12 and translated by Peng, Chaoqun and Hu, Guocheng

structure parameters (voltage — 10 kV, current 100 mA, $\Delta(2\theta) < 0.01°$).

3 RESULTS

3.1 *Morphology Observations*

Fig. 1 shows the cross-section morphology of a strip(R — contact surface; F — free surface). It is clear that the morphology feature of the strip is granular second phase particles distributing among columnar grain matrix. Most of the columnar grains ($d10 \sim 15\ \mu m$) run through the strip from the contact surface to the free surface. The distribution of the second phase particles among the columnar grains is non-uniform. And this non-uniformity is getting clearer and clearer from the contact surface to the free surface.

Fig. 1 Cross section morphology of strip

Figs. 2 and 3 show the TEM morphologies at positions close to the contact surface and the free surface, respectively. It can be seen that there exists second phase particles at all positions; and that the second phase particles close to the contact surface are smaller ($d20 \sim 100$ nm) and densier. Therefore, the smaller second phase particles at positions close to the contact surface are hard to distinguish. The second phase particles at positions close to the free surface are larger($\sim 100 - 200$ nm) and less densified.

The composition analyses made on the matrix and the second phase show that the second phase has the same composition as the matrix. This indicates that the second phase is also composed of near equiatomic Ni and Ti, see Figs. 4 and 5.

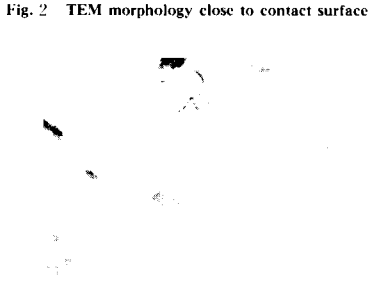

Fig. 2 TEM morphology close to contact surface

Fig. 3 TEM morphology close to free surface

After a heat treatment at 750 ℃ for 5 min followed by furnace cooling, the morphology of the strip is composed of equiaxed grains with diameters about 100 nm. The second phase particles are dissolved. This indicates that the second phase is unstable at 750 ℃ and it will transform into the *B*2 structure matrix.

3.2 *Structure Analysis*

Figs. 7 and 8 are the *a* diffraction patterns of the second phase along different crystallographic directions. The analyses indicate that these two patterns can be perfectly demarcated with $\bar{1}00$ and $\bar{1}10$ patterns of *fcc* stuctures, respectively. So

the second phase can be determined to be of *fcc* structure; and the lattice constant a_0 can be calculated by using the patterns to be 1.33 Å. Because no superlattice reflection appears, the Ni and Ti atoms in this phase are disordered.

By analysing the X-ray diffraction spectrum of the contact surface (Fig. 9), we found that besides the diffraction peaks of the B_2 structure matrix, there exists a weak diffraction peak between $(100)_{B_2}$ and $(110)_{B_2}$, which has an inter-planar spacing of 2.486 Å. By comparing this value with

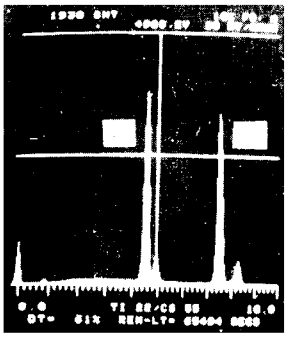

Fig. 4 Energy spectrum of matrix

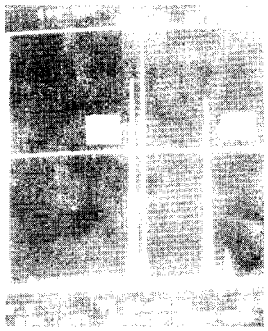

Fig. 5 Energy spectrum of second phase

Fig. 6 TEM morphology of strip after heat treatment at 750 ℃ for 5 min followed by furnace cooling

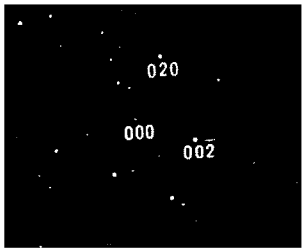

Fig. 7 [100] electron diffraction pattern of second phase

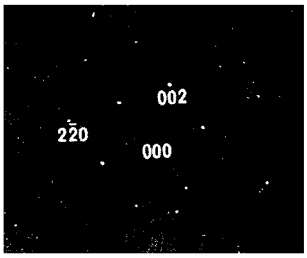

Fig. 8 [110] electron diffraction pattern of second phase

the structure parameter of the second phase determined from the electron diffraction patterns, we can believe this weak peak to be the (111) peak of the second phase. Becase the strongest diffraction peak of an *fcc* metal without preferred orientations is (111) peak, the lattice constant can be calculated to be $a_0 = 4.300$ Å according to the X-ray diffraction spectrum. This value agrees with that determined by the electron diffraction patterns. With regards to the fact that the precision of the lattice constant determined by the X-ray diffraction spectrum is better than that by the electron diffraction patterns, the former lattice constant should be more accurate.

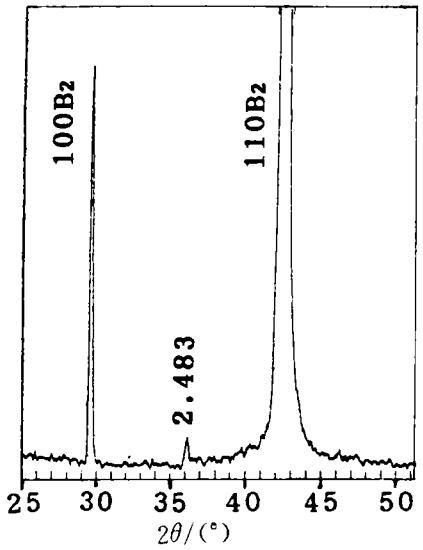

Fig. 9 X-ray diffraction pattern at position close to contact surface

4 DISCUSSION

At the present, the *fcc* second phase in the Ni-Ti alloy was first found. Therefore, the research on its formation mechanisms is of utmost importance. The second phase may form by two ways. The first is that it forms directly from the solidification of the liquidoid; the second is that it is transformed from the parent phase through solid phase change after the B_2 type parent phase has been formed. The discussion on these two possible formation mechanisms are as follows.

With regards to the thermodynamic conditions of its formation, the second phase has the same composition as the parent phase; but its structure is different from those of the parent phase (cubic CsCl sturcture)[1], *R* phase (rhombic structure)[2] and *M* phase (*B'* 19 monoclinic structure)[3] in the Ni-Ti alloy under common solidification conditions. This indicates that it is difficult for this *fcc* second phase to form under the common solidification conditions. Therefore, the second phase is unstable under near equilibrium state thermodynamically. This phase dissolves into the parent phase when heated at 750 C. This further confirms that the stability of the second phase is lower than that of the parent phase; and it is not easy for this phase to form from the parent phase through solid phase change. Therefore, the second phase should nucleate prior to the parent phase. Seen from the Ni-Ti equilibrium diagram, we know that there exists no other high temperature phases between the parent phase and the liquidoid[4]. Therefore, it is very likely that the second phase nucleates directly from the liquidoid. Because it is unstable thermodynamically, this phase must be a metastable phase. However, the formation of a metastable phase directly from the liquidoid requires that the melt reaches a very large overcooling degree, so that the free energies of the parent phase and the second phase can be lower than that of the molten Ni-Ti alloy simultaneously. Rapid solidification can satisfy this condition.

It cannot be clearly explained by only using thermodynamics why the melt does not completely solidify out into the parent phase with lower free energy, but forms part of metastable phase with higher free energy. Therefore, it is necessary to find the internal kinetic cause for the formation of the metastable phase. The solidification of the parent phase and the metastable phase is a process of nucleation and growth; and the nucleation is the prerequisite of the growth. By comparing the crystal structures between the parent phase and the metastable phase, with regards to their atomic arrangements, the Ni and Ti atoms in the parent phase must be arranged in ordered B_2 structure; and those in the *fcc* metastable phase are disordered. Therefore, the atomic rearrangements for the nucleation of the metastable phase are more arbitrary,

then it is easier for the metastable phase to nucleate. If the thermodynamic conditions for its formation in the overcooled melt is satisfied, the metastable phase should nucleate preferentially.

Most of the structure in Figs. 1～3 is the parent phase. This indicates that the formation of the metastable phase does not completely hinder the formation of the parent phase; and this can be explained from their difference in growth rates: although the metastable phase nucleate prior to the parent phase, the later can also nucleate and grow under the experimental conditions. Due to the fact that the free energy of the parent phase is lower than that of the metastable phase, the equilibrium temperature of free energy between the parent phase and the liquidoid is higher than that between the metastable phase and the liquidoid. Therefore, the nuclei of the parent phase has large overcooling degree; and the latent heat released from solidification has less influence on their growth rates. On the contrary, the overcooling degree of the metastable phase is smaller and the latent heat released from solidification during its growth further reduces the overcooling in the liquid-solid front edge. Consequently, the growth rate of the metastable phase is lower because of the limitation of the overcooling degree after its nucleation. The parent phase grew at a higher rate under the temperature gradient from the contact surface to free surface, then formed the morphologies as shown in Figs. 1～3.

5 CONCLUSIONS

(1) Under a cooling rate of about 2×10^5 K/s, there appears a granular *fcc* metastable phase in the Ni-Ti alloy with the lattice constant $a_c = 4.300$ Å. This phase has the same composition as the parent phase; and it is also composed of near equiatomic Ni and Ti.

(2) The sizes of the second phase in the strip vary along the thickness. The second phase particles at positions close to the contact surface are smaller and densier. As the position moves toward the free surface, the sizes of the second phase particles become larger and their distribution gets less densified.

(3) The second phase is believed to form directly from the liqudoid by a preliminary analysis. But its formation mechanism needs to be further studied.

REFERENCES

1 Jackson, C M; Wangner, H J; Wasilewski, R J. NASA-SP5110, 1972, 5.
2 Chandra, K; Purdy, G P. J Appl phys, 1986, 39: 2049.
3 Kudoh, Y; Tokonami, M. Acta Metall, 1985, 33 (11): 2049.
4 Margolin, H; Ence, E; Nulsen, J P. Trans AIME, 1953, 197: 243.
5 Wishida, M; Wayman, C M. Met Trans, 1987, 18 (5): 785.
6 Nishida, M; Honma, T. Scripta Metall, 1985, 19: 983.
7 Igharo, M; Wood, J V. Mater Sci Eng, 1988, 98: 443.

(*from page 76*)

REFERENCES

1 Schillmoller, C M. Chemical Engineering, 1980, (3): 161.
2 Elliott, P *et al*. Corrosion, 1988, 44: 541.
3 Hauffe, K; Hinrichs, J. Werkst Korros, 1970, 21: 954.
4 Matlis, Y B *et al*. In: Proceedings of 3rd International Congress on Metallic Corrosion, vol. 4, Moscow, 1966. 261.
5 Lee, Y Y; McNallan, M J. Metall Trans, 1987, 18A: 1099.
6 Tedmon, C S; J Electrochem Soc, 1966, 113: 766.
7 Kubaschewski, O; Alcock, C B. Metall Thermochem, 5th Edition, Pergamon Press, 1977. 387.
8 Singh, C T; Balk, P. J Electrochem Soc, 1978, 125: 153.
9 Dieckmann, R Z. Phik Chem, 1977, 107: 189.